Mullite macro-needles for reinforcement of refractory castables

A. Mocciaro[1], A. Cimas[1], N. M. Rendtorff[1,2], A. N. Scian[1,2]*
[1]Centro de Tecnología de Recursos Minerales y Cerámica (CIC-CONICET La Plata), Camino Centenario y 506-1897, M.B Gonnet, Argentina
[2]Universidad Nacional de La Plata, Facultad de Ciencias Exactas, Departamento de Química, La Plata, Argentina

Abstract

Ceramic macro-needles incorporation as reinforcement in commercial refractory castable was studied. Ceramic macro-needles (Ø2x20 mm) were made from kaolinite clay and gibbsite to obtain mullite as the main crystalline phase. Specimens with the ceramic reinforcement were evaluated by compression after being treated at two temperatures (815 and 1400 °C). The results were compared with those obtained using the same commercial concrete but reinforced with steel fibers and without reinforcement. Compression values presented by specimens with ceramic macro-needles were 74% and 50% higher than specimens with steel fibers after exposition to 815 and 1400 °C, respectively. Based on these results, it was established that ceramic macro-needles are a feasible solution to improve the mechanical resistance of castables exposed to high temperatures.
Keywords: refractories, fibers, mechanical properties.

INTRODUCTION

Refractory castables are materials widely used in industrial applications because they withstand different chemical environments and high temperatures. Refractory castables at the moment of the installation are mixed with a liquid, generally water, and popped, vibrated, poured, or pneumatically shot into the required form and consolidated *in situ* by hydraulic or chemical setting. The main advantages are that they reduce the number of joints, the material is sintered during service so the sintering process before installation is eliminated and its application is fast which reduces the halt of the plant [1, 2]. Previous works have already studied the behavior of refractory castables based on alumina with stainless steel fiber reinforcement [3-5]. Steel fibers improve the mechanical properties of the castables, especially compressive strength, impact strength, and toughness [6]. The main disadvantage is that after treatments at 750 °C the steel fibers start to lose their mechanical properties, they become soft and they oxidize [7]. Moreover, steel fibers contribute to accelerating the heating of the castable and can promote internal micro-cracking because of thermal incompatibility with the refractory castable matrix [8-10].

An option to reinforce refractory castables that are exposed to high temperatures (>800 °C) could be the incorporation of mullite macro-needles instead of steel fibers. Mullite is an aluminosilicate ($3Al_2O_3.2SiO_2$) widely studied and used due to its favorable thermal and mechanical properties [11-14]. A well-known way to obtain mullite is by thermal reaction of kaolinitic clays [15, 16]. When kaolinitic clay is heated above 1400 °C, mullite (primary mullite) and SiO_2 are formed. The amount of SiO_2 in excess can react by adding extra alumina to form secondary mullite; alumina addition can increase the final amount of mullite and reduce the amount of glass phase [17-19]. The objective of the present research is to evaluate the possibility of using mullite macro-needles as reinforcement in refractory concrete. Mullite macro-needles were processed from the thermal treatment of a kaolinitic clay and gibbsite. First, the microstructure and mechanical strength of macro-needles were characterized. Then, the macro-needles were added to a commercial refractory castable, analyzed, and compared to the case of the castable reinforced with steel fibers.

EXPERIMENTAL

Raw materials: kaolinitic clay from Arcamin (Buenos Aires, Argentina) and gibbsite (Minas Gerais, Brazil) were used as starting materials to make macro-needles. The chemical composition of the kaolinitic clay is presented in Table I. The gibbsite characterization can be found in a previous work [20] where $Al(OH)_3$ was determined by the X-ray diffraction technique as the only crystalline phase in the sample. In addition to kaolinitic clay composition analysis, loss on ignition (LOI) of the gibbsite was also carried out with the objective of determining the content of Al_2O_3. The gibbsite was dried for 24 h at 110 °C, and then it was fired at 1000 °C for 1 h in an electrical furnace with a 5 °C.min^{-1} heating rate. Gibbsite LOI was 34.54 wt%, consequently, the content of Al_2O_3 was determined as 65.46 wt%. According to the kaolinitic clay chemical composition (Table I) and the amount of alumina in the gibbsite, the relation between kaolinitic clay and gibbsite (40.7 and 59.2 wt%, respectively) necessary to obtain mullite ($3Al_2O_3.2SiO_2$) was calculated after thermal treatment.

**anamocciaro@cetmic.unlp.edu.ar*
https://orcid.org/0000-0001-7764-067X

Table I - Chemical composition (wt%) of the kaolinitic clay.

SiO_2	Al_2O_3	K_2O	TiO_2	MgO	Fe_2O_3	CaO	Others	LOI
51.76	35.08	3.15	1.41	0.81	0.42	0.15	0.20	7.01

LOI: loss on ignition.

Macro-needle preparation: the mixture of kaolinitic clay and gibbsite was ball milled using an alumina jar and milling media in a wet condition with 0.2 wt% of a dispersant (Dolapix PC 67) [21]. The mixture with 60% of humidity was molded into Ø2 mm rods using a ram-type extruder. The extruded green bodies were dried at room temperature for 24 h then dried at 110 °C for another 24 h and fired in an electric furnace with a heating rate of 5 °C.min^{-1} up to 1550 °C with 3 h soaking in air atmosphere [22]. After heat treatment, the rods were cut to obtain ~20 mm long macro-needles, the same length as the steel fibers.

Reinforced refractory castables preparation: a commercial refractory castable (Carboxite 66, Morgan Thermal Ceramics) containing a high amount of alumina (~90 wt%) was used. Refractory castables samples with two types of reinforcement were made: samples with macro-needles after the thermal process (HC) and samples with steel fibers (HM). In addition, samples of refractory concrete without reinforcement (H) were made as a reference. Commercial corrugated type steel fibers 20x1.2x0.5 mm^3 in size (WCR, Shanghai Shwitcom, China) were employed for the HM samples. These fibers presented one rough surface and one smooth surface, resulting in a large interface area between the fiber and the castable [23]. 3 wt% of steel fibers were incorporated into the castable as reinforcement in the HM samples. On the other hand, for the HC samples, 1.5 wt% of macro-needles was added. These contents were calculated based on the apparent density of the macro-needles and steel fibers, to reach 1% of the total volume occupied with reinforcement material in each case [8, 24]. Castables preparation was carried out in a Hobart-type laboratory mixer with a capacity of 5 L. The dry castable initially was mixed for 1 min followed by the addition of the macro-needles or steel fibers, depending on the sample. Mixing continued for 3-5 min to ensure uniform distribution, then 9 wt% of water was added according to the technical sheet of the castable, and mixing continued again for 1-2 min. The fresh castable mixtures were cast into prismatic-shaped molds (50x50x250 mm^3) and consolidated using a vibrating table according to ASTM C862 standard [25]. All test specimens were demolded after 24 h of casting and then cured at 110 °C for another 24 h. The specimens were fired in an electric furnace with a heating rate of 2 °C.min^{-1} with a soaking time of 300 min at two different maximum temperatures, 815 or 1400 °C, according to the API 936 standard [26]. Fig. 1 illustrates refractory castables manufacturing.

Macro-needles characterization: in order to determine the particle size distribution of the mixture of kaolinitic clay and gibbsite, after the milling process a laser diffraction particle size analysis was performed (Hydro 2000G, Malvern) using distilled water as the suspension medium. The mineralogical composition of the macro-needles after firing was determined by X-ray powder diffraction (XRD) with a diffractometer (D2 Phaser, Bruker) using CuKα radiation operating at 40 kV and 30 mA. XRD patterns were analyzed with a multipurpose profile-fitting program (FullProf v.5.80-2016) including Rietveld refinement to perform phase quantification of crystalline and amorphous phases [27]. The amorphous phase was quantified by the Le Bail approach, in which this phase is introduced in the refinement as crystalline silica with extremely low crystallite size [28-30]. The apparent density and open porosity of the

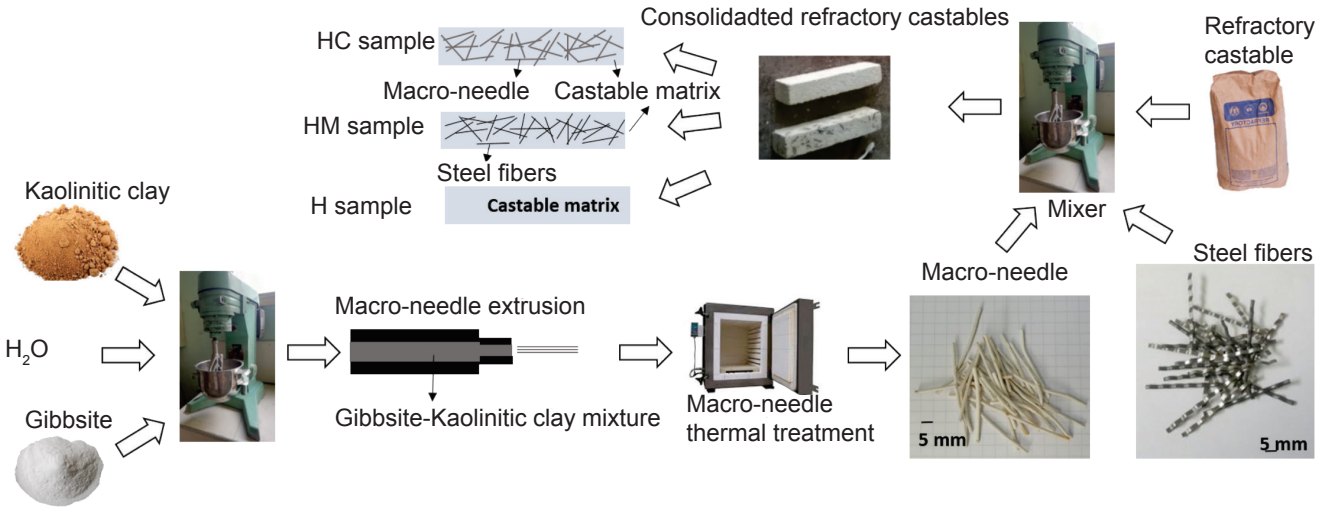

Figure 1: Schematic representation of the reinforced refractory castables manufacturing.

sintered macro-needles were evaluated by the Archimedes immersion method in water. A mercury intrusion test was also performed using a mercury porosimeter (Pascal 440, Thermo Scientific). The mechanical characterization of individual macro-needle was carried out by a 3-point bending test in a universal mechanical testing machine (mod. 5985, Instron, USA) at a constant crosshead speed of 0.5 mm.min^{-1}. Flexural strength (σ_f) was calculated by [31]:

$$\rho_f = \frac{8.F.I}{\mu.d^3} \quad (A)$$

where F is the maximum stress load, l is the distance between support points, and d is the diameter of the specimens. At least 8 samples were evaluated and the average of results was informed. Finally, microstructure analysis was performed by scanning electron microscopy (SEM, JCM-6000, Jeol).

Reinforced and not reinforced refractory castables characterization: samples HC and HM were characterized following the API 936 standard. The apparent density after exposition at 815 or 1400 °C was determined by the volumetric size and weight measures. The permanent linear change (PLC) was calculated by measuring the dimensions of specimens before and after firing. In order to analyze the microstructure of the refractory castables, SEM images were taken for HC and HM samples after thermal treatment at 815 °C. Additionally, mechanical strength was evaluated by uniaxial compression in a universal mechanical testing machine (mod. 5985, Instron). The uniaxial compressive test was carried out on samples (50x50x50 mm^3) fired at 815 or 1400 °C at a constant crosshead speed of 0.5 mm.min^{-1}, with steel plates. Mechanical characterization was made according to ASTM C133 standard [32]. The results reported are the average measurements taken over 5 test pieces per each material.

RESULTS AND DISCUSSION

Textural and mechanical properties of the macro-needle

Fig. 2 shows the particle size distribution curve of the kaolinitic clay-gibbsite mixture after the milling process. Fine particle size was confirmed, particularly a bimodal distribution was observed with the first peak between 1 and 10 μm and a second peak between 50 and 110 μm. Table II shows the statistical parameters of the distribution.

Macro-needle XRD pattern is shown in Fig. 3. Mullite accompanied by alumina was identified as crystalline phases in the macro-needle. The result of Rietveld quantification with R_{wp} residual is presented in Table III. The R_{wp} parameter is used for assessing the quality of the Rietveld refinement. The obtained values were acceptable and similar to others found in the literature for similar materials [33, 34]. The amount of mullite was 76.8 wt% and the amount of amorphous phase was 22.0 wt%; this showed that the mullitization was not complete. The high amount of amorphous phase could be related to the content of K_2O in the chemical composition of the clay (Table I) which is a glass modifier oxide [35]. The presence of alkalis in the clay affects the mullite formation and results in mullite grains embedded in an aluminosilicate glass matrix [36].

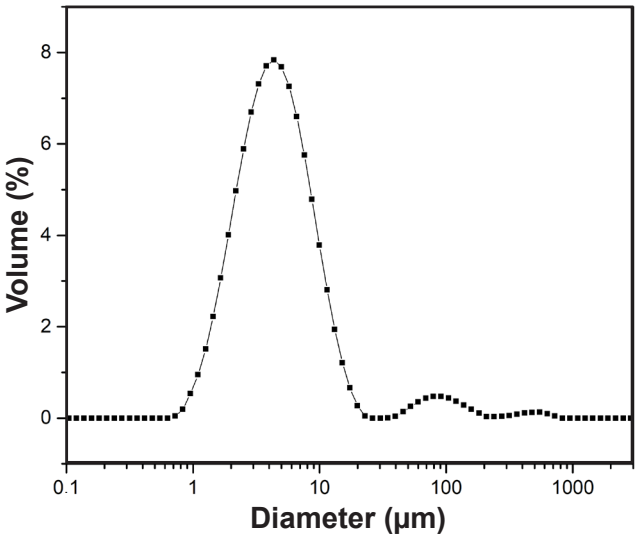

Figure 2: Particle size distribution curve for the kaolinitic clay-gibbsite mixture after milling.

Table II - Maximum diameter for 10%, 50%, and 90% of the particles.

$d_{0.1}$ (μm)	$d_{0.5}$ (μm)	$d_{0.9}$ (μm)
1.75	4.15	10.55

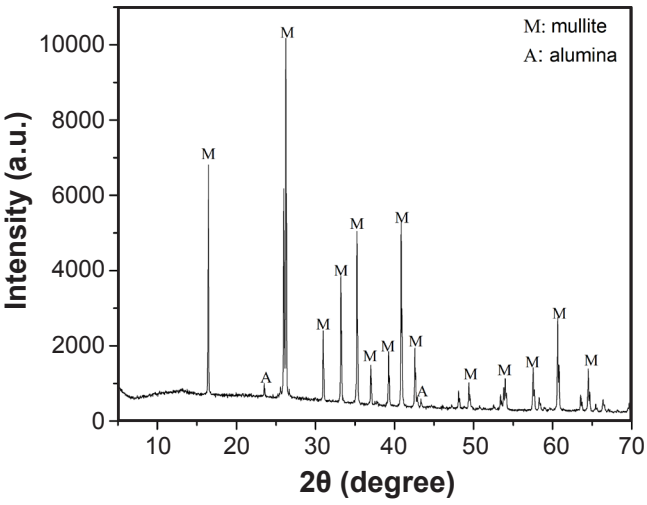

Figure 3: XRD pattern of fired macro-needle.

The apparent density of the macro-needle was 2.6 g.cm^{-3} and the open porosity measured by Archimedes method was 8%. The pore size distribution by Hg intrusion was d_{10} 0.13 μm, d_{50} 0.62 μm, and d_{90} 10.19 μm. These results were similar to those reported in the literature for mullite ceramics [37, 38]. The physical parameters and the Rietveld quantification (Table III) revealed that thermal treatment generated the formation of mullite. The flexural strength of

Table III - Identified crystalline phases, formula, PDF files, and Rietveld quantification results of the macro-needle.

Crystalline phase	Formula	PDF file	Rietveld method-R_{wp} 17.7 (wt%)
Mullite	$Al_2O_3.2SiO_2$	01-079-1453	76.8 (8)
Alumina	Al_2O_3	01-088-0826	1.2 (8)
Amorphous phase	Silica and alumina-based	Le Bail method	22.0 (8)

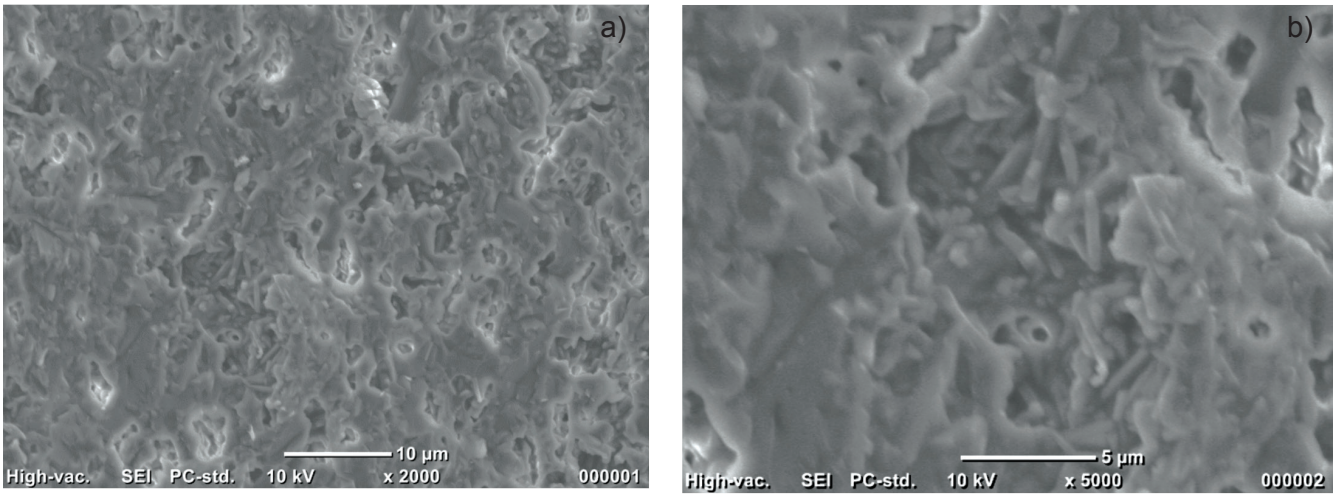

Figure 4: SEM images of the fracture surface of the mullite macro-needle after firing at 1550 °C.

the sintered macro-needles was 160±20 MPa; similar values have already been reported in the literature [11, 17]. Fig. 4 shows SEM images of the fracture surface of the macro-needle. As can be seen, the microstructure was dense with submicrometer grains and some pores, in agreement with the sintering process and comparable to previous studies in similar materials [36, 39]. Some mullite grains with acicular forms (diameter lower than 1 µm) were observed. Thermal decomposition of kaolinitic clay produced primary mullite and amorphous silica in a liquid phase. Probably, the dissolution of the added alumina particles in the liquid phase generated the precipitation of secondary mullite grains [36, 40]. For this reason and according to amorphous phase quantification by XRD (Table III), mullite grains embedded in a glassy matrix were observed [40]. On the other hand, alumina grains were not possibly observed because of their low amount, as determined in the XRD analysis.

Evaluation of castables properties

Table IV shows the results for density and PLC of H, HC, and HM samples exposed at 815 and 1400 °C. Density values decreased for the higher temperature in all samples, which was related to water loss of the starting materials. In this regard, the hydrated phases of calcium aluminate cement (CAC) have a series of reactions with associated water loss [2, 41, 42]. $CaO.Al_2O_3.10H_2O$ (CAH_{10}) and $2CaO.Al_2O_3.8H_2O$ (C_2AH_8) are metastable phases that are dehydrated forming $3CaO.Al_2O_3.6H_2O$ (C_3AH_6) and $Al_2O_3.3H_2O$ (AH_3) with water release below 200 °C. At 240-370 °C, C_3AH_6 is dehydrated forming $12CaO.7Al_2O_3.H_2O$ ($C_{12}A_7H$), $CaO.H_2O$, and water release. Above 300 °C, AH_3 has a two-step dehydroxylation process. First, it transforms into boehmite [AlO(OH)] between 300 and 400 °C, with water release. Later, AlO(OH) loose water between 400 and 500 °C forming amorphous Al_2O_3 [43, 44]. Furthermore, $CaO.H_2O$ is dehydrated at ~450 °C and $C_{12}A_7H$ is dehydrated in $12CaO.7Al_2O_3$ ($C_{12}A_7$) at ~750 °C. The PLC values decreased between 110 and 815 °C and then increased at 1400 °C. Contractions are related to thermal transformations with associated water loss; on the other hand, the expansion presented in the samples was associated with the generation of CA_6 ($CaO.6Al_2O_3$) as a product of the thermal reaction between the cement phases [CA ($CaO.Al_2O_3$) and CA_2 ($CaO.2Al_2O_3$)] at 1400 ° C [45].

In Fig. 5 SEM images of the HC and HM samples after thermal treatment at 815 °C are shown. The microstructure developed by the refractory castables with reinforcement was observed on a microscopic scale. The macro-needles and the steel fibers were embedded in the refractory castable matrix. This matrix was formed by grains with a wide particle size distribution from a microscopic scale to 3 mm. No differences were observed between the HM and HC samples; both castables settled around the reinforcement macro-fiber. It was expected that the steel fibers and macro-needles if they had good mechanical resistance, would generate improvements in the mechanical resistance of the refractory castable.

Cold compressive strengths of the refractory castables after firing at 850 and 1400 ºC are shown in Fig. 6. Mechanical strength of all samples presented similar values to others reported in the literature [5, 46]. After being fired

Table IV - Density and permanent linear change (PLC) values of the H, HC, and HM samples after thermal treatment.

Temperature (°C)	Density (g.cm^{-3})			PLC (%)		
	H	HC	HM	H	HC	HM
815	2.56 (3)	2.51 (3)	2.63 (1)	-0.14 (6)	-0.17 (1)	0.08 (8)
1400	2.53 (1)	2.27 (2)	2.39 (4)	2.00 (4)	3.18 (4)	4.00 (8)

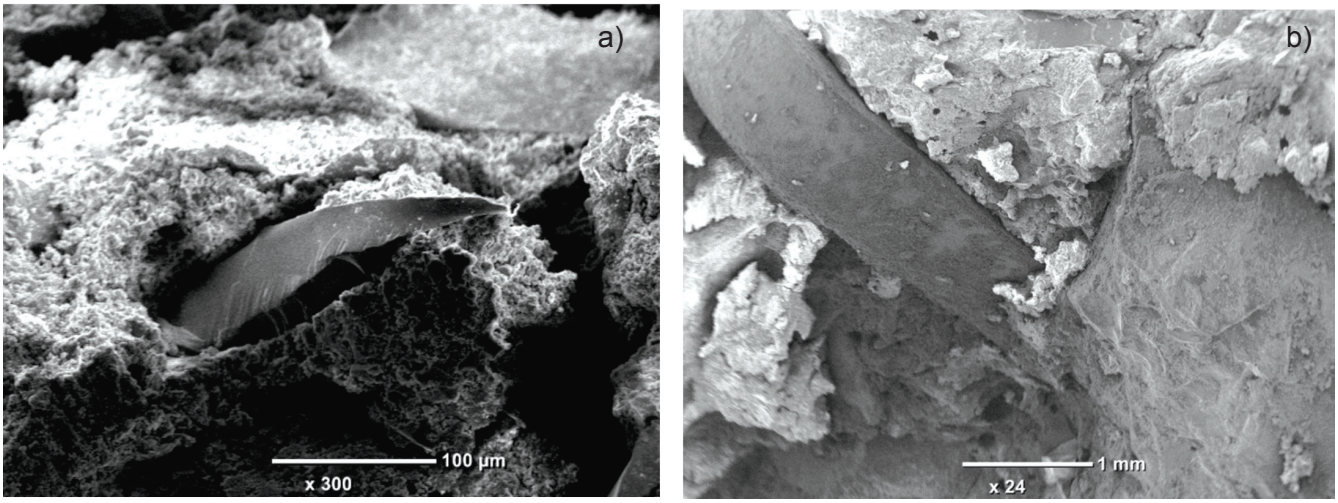

Figure 5: SEM images of the samples HC (a) and HM (b) after thermal treatment at 815 °C.

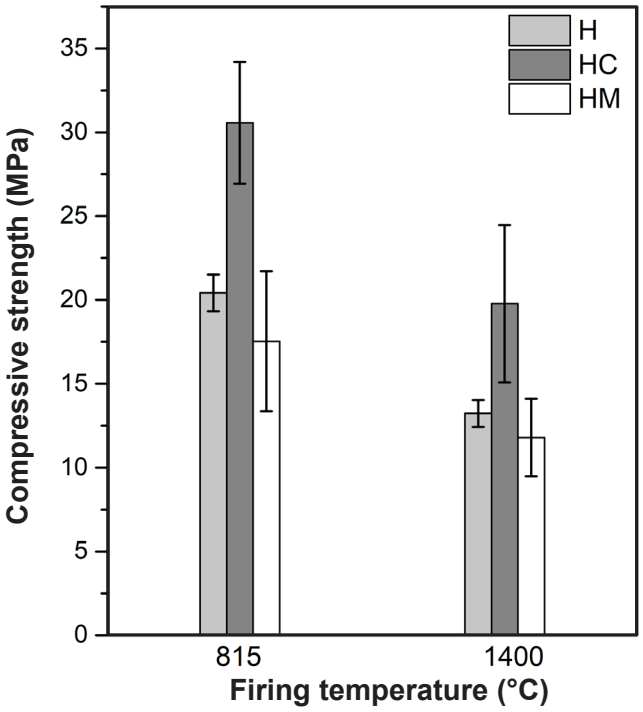

Figure 6: Cold compressive strength of H, HC, and HM samples after firing at 815 and 1400 °C.

at 1400 °C, all the samples had decreased their compressive strength by around 30% with respect to the strength values after being fired at 815 °C. This decrease in mechanical behavior could be related to the concrete matrix rather than to the reinforcement material. However, ceramic-reinforced concrete showed improvement compared to unreinforced concrete. If the two reinforcement materials are compared, it is observed that the HC samples presented a compressive strength of over 74% higher than that of HM samples after firing at 815 °C and ~50% higher after firing at 1400 °C. The degradation process of the steel fibers found in the literature [7] was evidenced by these lower values of mechanical resistance of the HM samples. According to the literature, an understanding of mechanical behavior, with other thermophysical parameters, allows describing the thermal shock behavior of ceramics [47-50]. This behavior indicated that mullite macro-needles could be a good option to use as reinforcements in materials exposed to thermal stress.

CONCLUSIONS

Ceramic (mullite) macro-needles for refractory castables reinforcement were processed, characterized, and tested in a model castable. The macro-needles were extruded from a kaolinitic clay-gibbsite mixture and after a thermal treatment, mullite was the main crystalline phase. Textural and mechanical characterization of the macro-needles confirmed the mullite formation with a dense refractory fine-grained microstructure. The performance of the macro-needles as reinforcement in a refractory castable (HC) was evaluated and compared to refractory castable with steel fibers as reinforcement (HM) and with concrete samples without reinforcing material. Refractory castables with macro-needles presented the highest values of compressive

strength after exposure to two temperatures (815 and 1400 °C). All the samples showed a decrease in their mechanical behavior between 815 and 1400 °C, which could be related to the concrete matrix rather than the reinforcement material. In addition, the HC sample after heating at 815 °C improved 74% its compressive strength in comparison to the HM sample, and after heating at 1400 °C HC sample presented 50% higher compressive strength than the HM sample. These differences can be explained by the degradation at high temperatures of the steel fibers reported in the literature. Finally, based on the refractoriness of the macro-needles formed by mullite and alumina as crystalline phases, it was concluded that macro-needles could be used as reinforcement in refractory castables to improve their mechanical strength in applications with thermal stress due to high temperature during service.

ACKNOWLEDGMENTS

This work was partially supported by Facultad de Ciencias Exactas, Universidad Nacional de La Plata (UNLP, X-877, and X-904), and CETMIC. AM, NMR, and AS are members of CONICET. The authors also wish to thank Diego Richard and Susana Conconi for the final comments on the manuscript.

REFERENCES

[1] M.H. Moreira, S.D. Pont, R.F. Ausas, A.P. Luz, T.M. Cunha, C. Parr, V.C. Pandolfelli, Ceram. Int. **47**, 20 (2021) 28086.
[2] W.E. Lee, W. Vieira, S. Zhang, K.G. Ahari, H. Sarpoolaky, C. Parr, Int. Mater. Rev. **46**, 3 (2001) 145.
[3] A. Meddah, L. Belagraa, M. Beddar, Procedia Eng. **108** (2015) 185.
[4] M. Talaei, D. Mostofinejad, Constr. Build. Mater. **289** (2021) 122854.
[5] C.M. Peret, V.C. Pandolfelli, Cerâmica **51**, 317 (2005) 1.
[6] C.H. Sump, J. Mater. Energy Syst. **6**, 4 (1985) 279.
[7] F.B. Varona, F.J. Baeza, D. Bru, S. Ivorra, Constr. Build. Mater. **159** (2018) 73.
[8] W.G. Bareiro F. de Andrade Silvia, E.D. Sotelino, Constr. Build. Mater. **240** (2020) 117881.
[9] M. Rigaud, K. Balamurugan, K. Samkaranarayanane, Adv. Sci. Technol. **45** (2006) 2278.
[10] G. Bernhart, F. Nazaret, T. Cutard, Mater. Werkst. **39**, 4-5 (2008) 317.
[11] H. Schneider, J. Schreuer, B. Hildmann, J. Eur. Ceram. Soc. **28**, 2 (2008) 329.
[12] R. Torrecillas, J.M. Calderón, J.S. Moya, M.J. Reece, C.K.L. Davies, C. Olagnon, G. Fantozzi, J. Eur. Ceram. Soc. **19**, 13-14 (1999) 2519.
[13] M. Hammidouche, N. Bouaouadja, C. Olagnon, G. Fantozzi, Ceram. Int. **29**, 6 (2003) 599.
[14] N.M. Rendtorff, L.B. Garrido, E.F. Aglietti, Ceram. Int. **34**, 8 (2008) 2017.
[15] L. Andrini, M.R. Gauna, M.S. Conconi, G. Suarez, F.G. Requejo, E.F. Aglietti, N.M. Rendtorff, Appl. Clay. Sci. **124-125** (2016) 39.
[16] A.K. Chakraborty, *Phase transformation of kaolinite clay*, Springer, India (2014).
[17] C.Y. Chen, G.S. Lan, W.H. Tuan, J. Eur. Ceram. Soc. **20**, 14-15 (2000) 2519.
[18] J. Temuujin, K.J.D. Mackenzzi, M. Schmücker, H. Schneider, J. Mcmanus, S. Wimperis, J. Eur. Ceram. Soc. **20**, 4 (2000) 413.
[19] J. Martín Marquez, J.M. Rincón, M. Romero, J. Eur. Ceram. Soc. **30**, 7 (2010) 1599.
[20] A.X. Moreno Eraso, "Obtención tecnológica de mullita a partir de arcillas y caolines refractarios argentinos, y alúmina calcinada o alúminas hidratadas", Dr. thesis, Un. Nac. La Plata (2014).
[21] F. Nunes, A.G. Lamas, M. Almeida, H.M.M. Diz, J. Mater. Sci. **27**, 24 (1992) 6662.
[22] C. Sadik, I.E.E Amranni, A. Albizane, J. Asian Ceram. Soc. **2**, 4 (2014) 310.
[23] J. Ran, T. Li, D. Chen, L. Shang, W. Li, Q. Zhu, Structurs **34** (2021) 1890.
[24] S.A. Bernal, J. Bejarano, C. Garzón, R. Mejía de Gutiérrez, S. Delvasto, E.D. Rodríguez, Compos. B Eng. **43**, 4 (2012) 1919.
[25] ASTM C08, "Practice for preparation refractory concrete specimens by casting", Am. Soc. Test. Mater. (2003).
[26] API Std 936, "Refractory installation quality control-inspection and testing monolithic refractory linings and materials", Am. Pet. Inst. (2004).
[27] H.M. Rietveld, J. Appl. Crystallogr. **2**, 2 (1969) 65.
[28] A. Le Bail, J. Non-Cryst. Solids **183**, 1-2 (1995) 39.
[29] M.S. Conconi, M.R. Gauna, M.F. Serra, G. Suarez, E.F. Aglietti, N.M. Rendtorff, Cerâmica **60**, 356 (2014) 524.
[30] A. Mocciaro, M.S. Conconi, N.M Rendtorff, A.N. Scian, J. Therm. Anal. Calorim. **144**, 4 (2021) 1083.
[31] P. Alander, L. Lassila, P. Vallittu, Dent. Mater. **21**, 4 (2005) 347.
[32] ASTM C133, "Standard test methods for cold crushing strength and modulus of rupture of refractories", Am. Soc. Test. Mater. (2003).
[33] M.S. Conconi, M. Morosi, J. Maggi, P.E. Zalba, F. Cravero, N.M. Rendtorff, Cerâmica **65**, 374 (2019) 227.
[34] M.F Serra, M.S. Conconi, M.R. Gauna, G. Suarez, E.F. Aglietti, N.M. Rendtorff, J. Asian Ceram. Soc. **4**, 1 (2016) 61.
[35] M.F. Serra, M.S. Conconi, G. Suarez, E.F. Aglietti, N.M. Rendtorff, Cerâmica **59**, 350 (2013) 254.
[36] W.E. Lee, G.P. Souza, C.J. McConville, T. Tarvornpanich, Y. Iqbal, J. Eur. Ceram. Soc. **28**, 2 (2008) 465.
[37] M.M.S. Sanad, M.M. Rashad, E.A. Abdel-Aal, M.F. El-Shahat, Ceram. Int. **38**, 2 (2013) 1547.
[38] J. Bai, Ceram. Int. **36**, 2 (2010) 673.
[39] P.S. Behera, S. Bhattacharyya, Mater. Today Commun. **26** (2021) 101818.
[40] P.J. Sánchez-Soto, D. Eliche-Quesada, S. Martínez-

Martínez, E. Garzón-Garzón, L. Pérez-Villarejo, J.M. Rincón, Mater. Lett. **223** (2018) 154.
[41] A. Hidalgo, J.L. García, M.C. Alonso, L. Fernández, C. Andrade, J. Therm. Anal. Calorim. **96**, 2 (2009) 335.
[42] M.A. Maaroufi, A. Lecomte, C. Diliberto, O. Francy, P. Le Brun, J. Eur. Ceram. Soc. **31**, 3 (2015) 1637.
[43] S. Maitra, S. Bose, N. Bandyopadhyay, A. Roychoudhury, Ceram. Int. **31**, 3 (2005) 371.
[44] M. Laaskou, G. Margomenou-Leonidopoulou, V. Balek, J. Therm. Anal. Calorim. **84**, 1 (2006) 141.
[45] A.G. Tomba Martinez, A.P. Luz, M.A.L. Braulio, E.Y. Sako, V.C. Pandolfelli, J. Eur. Ceram. Soc. **37**, 15 (2017) 5023.
[46] W.G. Bareiro, F. de Andrade Silva, E.D. Sotelino, F.M. Gomes, Constr. Build. Mater. **187** (2018) 1214.
[47] G.A. Schneider, Ceram. Int. **17**, 6 (1991) 325.
[48] W.D. Kingery, J. Am. Ceram. Soc. **38**, 1 (1955) 3.
[49] N.M. Rendtorff, E.F. Aglietti, in "Encyclopedia of thermal stresses", Springer (2014) 5119.
[50] N.M. Rendtorff, E.F. Aglietti, Mater. Sci. Eng. A **527**, 16-17 (2010) 3840.
(Rec. 13/04/2022, Rev. 20/06/2022, 27/07/2022, Ac. 01/08/2022)